2010 NDIA GROUND VEHICLE SYSTEMS ENGINEERING AND TECHNOLOGY SYMPOSIUM
MODELING & SIMULATION, TESTING AND VALIDATION (MSTV) MINI-SYMPOSIUM
AUGUST 17-19 DEARBORN, MICHIGAN

A STATISTICS-BASED DAMAGE MODEL THAT ACCOUNTS FOR SCALE EFFECTS

Arthur L. Gurson
Modeling & Simulation Department
Concurrent Technologies Corporation
Johnstown, PA

ABSTRACT

In this context, a damage model is a mathematical algorithm that is used to predict if and when in a given loading history a structure will fail by ductile fracture. Increments in a damage parameter are related to strain increments and state of stress. The damage model would operate as part of a numerical simulation, or separately on an output file. A scale effect in ductile fracture is widely recognized from test data, where a large structure tends to fail at lower strain than a smaller structure that is geometrically similar and of the same material. Most damage models are not scale sensitive, and when they are calibrated to data from small laboratory specimens, they will tend to over-predict the performance (i.e., energy absorbing capability) of a larger structure. Another factor is scatter in test results even when specimens are made with care to be as identical as possible. Both of these factors are addressed in the proposed statistics-based damage model. Scale effects and scatter become part of the actual material behavior, rather than perceived effects of variability in specimen preparation or test procedures. In addition, it is found that the statistical approach leads to improved calibration of the model for the effects of triaxiality and Lode parameter.

INTRODUCTION

Damage models are typically used to predict where in a given loading history a structure will fail. These models can be useful in ballistic and blast loading simulations. Some issues with widely used damage models are that they do not exhibit two phenomena seen consistently in test data; namely, scale effects and scatter. The scale effect is where a large structure tends to fail at lower strain than a smaller structure that is geometrically similar and of the same material. Test results of strain to failure typically show significant scatter, even when specimens are made with care to be as identical as possible in material and geometry.

When most widely used damage models are calibrated to data from laboratory specimens that are much smaller than a given structure, the damage models tend to over-predict the performance (i.e., energy absorbing capability) of that structure. A partial solution has been to use test data from large scale tests, but these are more difficult, expensive, and time consuming to perform than laboratory scale tests. Other approaches include use of strain gradients and length scales. None of these address the issue of scatter. We believe that we have found a better way to address these issues, by using a statistics-based damage model. It can be calibrated using data from laboratory scale tests, with perhaps some confirmatory data from larger scale tests.

The method is based on Weibull Statistics, with strain-to-failure as the independent variable. Damage is expressed in terms of a Probability of Survival (P_S), which starts at a value of 1 and decreases as plastic strain is accumulated. A scale factor appears in the formulation that increases with material volume and with the variability of the failure data, so for a given stress-strain history, a larger volume will have a lower value of P_S. Scale effects and scatter become part of the actual material behavior, rather than perceived effects of variability in specimen preparation or test procedures.

Other terms account for triaxiality and Lode angle. A statistical analog to the Johnson-Cook damage model is proposed.

Several examples are given that use published data of strain to failure vs. specimen geometry. It is shown that calibration for triaxiality and Lode angle make more sense when specimen geometry and gage volume are taken into account.

This work deals with the interaction of scatter and scale effects in ductile fracture through a statistical interpretation of the data. It is distinct from the type of deterministic scale effect seen in a body containing a crack, where a failure criteria such as energy release rate will be met at a lower stress when the scale of the body, and the length of the crack, are increased.

In this work, the approximations are made that the stresses in the gage volume are uniform, and are based on the initial geometry and plastic strain. It is recognized that calibration for FEA will improve when a specimen is modeled using a reasonable finite element grid, with incremental updates to geometry and plastic strain. Calibration would involve an adjustment of material parameters to minimize a function of the difference between test results and numerical results. Test results would be a relevant and easily measurable quantity, such as failure strain by reduction of area at the notch of a tensile specimen.

This paper presents part of the work done by *CTC* for the Naval Surface Warfare Center (Carderock Division) ACMII Program. A viewgraph summary can be accessed using reference [1].

START AND FINISH

Before the detailed analysis, it is useful to look at an example of a damage model that is currently in wide use, and see how our end product looks in comparison. The Johnson-Cook damage model [2] computes increments to a damage parameter that are based on strain increment and stress state. Increments are computed and summed separately for each element or integration point in a structure. Failure is said to occur when the value of the damage parameter at any point in the structure reaches a value of 1.

$$\varepsilon_F = \left[D_1 + D_2 \exp(D_3 \eta)\right]\left[1 + D_4 \ln\left(\frac{\dot{\varepsilon}^p}{\dot{\varepsilon}_0}\right)\right](1 + D_5 T_H) \quad (1)$$

$$T_H \equiv \text{Homologous Temperature}, = \frac{T - T_{ref}}{T_{melt} - T_{ref}}$$

$$D = \sum_{time}\left[\frac{\Delta\bar{\varepsilon}^p}{\varepsilon_F}\right], \text{ Failure when } D = 1$$

D_1 through D_5 are calibration coefficients, and D is a damage parameter. $\Delta\bar{\varepsilon}^p$ is an increment in equivalent plastic strain.

This is a deterministic model; the structure is intact until the criterion is met at any location, and then the structure has failed. It may be calibrated to mean values of samples, or to estimates of safe lower limits.

The statistics-based model has some similarities, but differs in that it computes a Probability of Survival (P_S), rather than a deterministic prediction of failure. The general form (minus the strain rate and temperature terms) is as below in equation 2. It expresses P_S for each element of a finite element grid, and for the total volume of the structure. Note the terms for element volume *V(k).* Also note terms for triaxiality (η) and Lode parameter (ξ).

$$\varepsilon_F = \exp(-C\eta) f_2(\xi)\varepsilon_0$$

(coefficient C and form of f_2 to be determined)

$$D(k) = \sum_{time}\left[\frac{\Delta\bar{\varepsilon}^p}{\varepsilon_F}\right] \quad \text{for element } k \quad (2)$$

$$V(k) = \text{volume of element } k$$

$$P_S(k) = \exp\left[-\left(\frac{V(k)}{V_0}\right)(D(k))^m\right],$$

$$P_S(total) = \prod_k P_S(k)$$

KEY ASSUMPTIONS AND APPROXIMATIONS

The material is isotropic, with standard Mises incompressible associative plasticity.

No strain rate effect is assumed unless otherwise noted.

For analysis purposes, the gage section of a specimen is treated as a single element, with uniform stress and strain.

The stress is calculated using the initial notch geometry and a modified Bridgman-type plasticity analysis.

As loading progresses, plastic strain increases, but the stress ratios (and thus triaxiality and Lode parameter) do not change.

The effective volume of the gage section is calculated using the area at the initial notch and the height of the gage section.

ANALYSIS

Weibull Statistics

This analysis uses the two parameter Weibull distribution [3-5]. The physical analogy is a single chain of a number (n) of links, which experiences a load (X) that increases until one of the links (and so the entire chain) fails. Each link sees the same load, but they all have different strengths. The strength of a link is described by a Probability of Survival that is a decreasing function of X, and the Probability of Survival of the chain is equal to the product of those values for the links.

For each link, $P_S(X) = \exp[-\Phi(X)]$,

$$\text{Use } \Phi(x) \approx \left(\frac{X}{X_0}\right)^m, \tag{3}$$

For a chain of n links,

$$P_S = \left\{\exp\left[-\left(\frac{X}{X_0}\right)^m\right]\right\}^n, = \exp\left[-n\left(\frac{X}{X_0}\right)^m\right]$$

The volume of material in the chain is proportional to n, so by analogy, for a body of volume V,

$$P_S(x) = \exp\left[-\left(\frac{V}{V_0}\right)\left(\frac{X}{X_0}\right)^m\right]$$
$$m \equiv \text{Weibull modulus} \tag{4}$$
$$X_0 \equiv \text{Weibull scale parameter}$$

Replace X by stress, and this is the form commonly used for failure of ceramics and composites. Here, plastic strain is used in place of X, as the independent variable.

Note that V_0 is an arbitrary scaling factor, such as 1 cubic inch or 1 mm^3. Take care when comparing different samples that the same value of V_0 is used.

Measurements of X at failure for a sample of n nominally identical specimens can be used to calibrate the equation. Results are arranged in ascending order, and a value of P_S is assigned to each that decreases as the failure strain increases.

$$\text{For } X_f(i), \quad i = 1 \text{ to } n, \tag{5}$$
$$P_S(i) = 1 - \frac{i - 0.5}{n}$$

Linearizing equation 4 by taking natural logarithms of both sides twice, and rearranging terms;

$$\left\{\ln\ln\left[\frac{1}{P_S(i)}\right] - \ln\left(\frac{V}{V_0}\right)\right\} = \tag{6}$$
$$m\ln[X_f(i)] - m\ln[X_0]$$

This is a set of n linear equations, that can be solved for optimal values of m and X_0 by linear regression. Using terms analogous to those in equation 6;

$$Y_i = a + bX_i, \quad i = 1 \text{ to } n \tag{7}$$
$$m = b, \quad X_0 = \exp\left(\frac{a}{m}\right)$$

(Note that for a given sample size, the range of Y is fixed, while the range of X depends on the scatter in the test data. When that scatter is small, the slope for Y vs. X will be large, and m will be large. It can be seen from equation 4, and later in equation 30, that the scale effect decreases as m increases.)

Next, postulate that there are several samples (n_S), the specimens within each sample are identical, and between samples, they are geometrically similar, but differ by a length scale. (Each sample will have its own gage volume.) The samples can have different numbers of specimens. Equations 5 and 6 can be written as follows to describe each sample:

$$\begin{aligned} &\text{Samples } k = 1 \text{ to } n_S, \\ &n(k) \text{ specimens in sample } k \\ &\text{For } X_f(i,k), \quad i = 1 \text{ to } n(k), \\ &P_S(i,k) = 1 - \frac{i - 0.5}{n(k)} \end{aligned} \tag{8}$$

Linearizing as in equation 6 gives

$$\begin{aligned} &\left\{ \ln\ln\left[\frac{1}{P_S(i,k)}\right] - \ln\left(\frac{V(k)}{V_0}\right) \right\} = \\ &m\ln\left[X_f(i,k)\right] - m\ln\left[X_0\right] \end{aligned} \tag{9}$$

Regression solutions for m and X_0 can be computed separately for each sample, or once for all of the samples together.

Gage Section Geometry and Stress State

Notched tensile specimens that undergo plastic yield in the gage section will generate transverse stresses that are related to the curvature at the notch and the normal stress across the notch. These stresses are zero at the free surface, and reach a maximum at the center. Approximate stress solutions for both the axisymmetric and plane strain cases are given in Bridgman [6]. Numerical solutions by Bao and Wierzbicki [7] for axisymmetry and by Gao [8] for plane strain suggest a correction factor of 1.4 on the variable part of the transverse stress. The Butterfly geometry is approximated as a shear stress added to the plane strain geometry.

Some examples of different notch geometries are shown in Figure 1 below. Note that for a given notch diameter or thickness, the approximate gage volume increases as the curvature decreases. For an unnotched specimen, the gage volume is determined by a specified gage length.

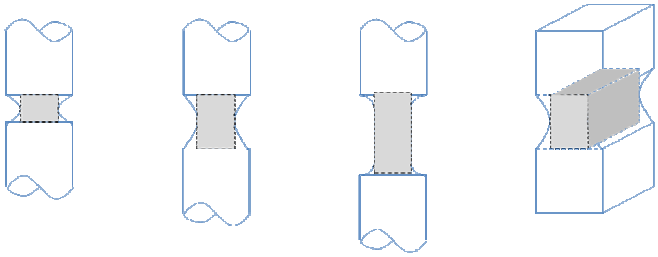

Figure 1. Axisymmetric and Plane Strain Specimens with Different Notch and Gage Geometries.

The details of the plasticity stress analysis can be found in Bridgman [6]. What follows is a summary of the results, with placement of the numerical factor [7 and 8]. Constant value approximations to the stresses will be calculated by computing an average over the cross section.

For the **axisymmetric** case;

$$\begin{aligned} &r = \text{radius at neck (surface value} = a), \\ &R = \text{radius of curvature at the notch} \\ &\sigma_Z(r=a) \equiv F, = \text{flow stress } (\bar{\sigma}) \text{ for this case} \\ &\text{Bridgman Factor: } f_r = \ln\left(\frac{a^2 + 2aR - r^2}{2aR}\right), \\ &\sigma_R = \sigma_\Theta = \bar{\sigma} f_r, \quad \text{and} \quad \sigma_Z = \bar{\sigma} * (1 + f_r) \end{aligned} \tag{10}$$

Average values over the cross section are:

$$\sigma(avg) = \frac{1}{\pi a^2}\int_0^a \sigma\, 2\pi r\, dr = \frac{2}{a^2}\int_0^a \sigma\, r\, dr$$

$$\sigma_R(avg) = \sigma_\Theta(avg) = \frac{2\bar{\sigma}}{a^2}\int_0^a f_r\, r\, dr, = \bar{\sigma}\, f_r(avg) \qquad (11)$$

$$\sigma_Z(avg) = \bar{\sigma} + \sigma_R(avg), = \bar{\sigma}\left[1 + f_r(avg)\right]$$

Carrying out the integral (CRC #377, [9]):

$$f_r(avg) = \left(1 + \frac{2R}{a}\right)\ln\left(1 + \frac{a}{2R}\right) - 1 \qquad (12)$$

And the triaxiality, with the numerical multiplier, is

$$\eta \equiv \frac{\sigma_H(avg)}{\bar{\sigma}} = 1.4\, f_r(avg) + \frac{1}{3} \qquad (13)$$

And in a similar process for **plane strain**, using Bridgman [6], and Gao [8];

$$x = \text{thkns direction} \quad (\text{Surface at } x = \pm a)$$

$$y = \text{width direction (zero strain)} \qquad (14)$$

$$z = \text{axial direction}$$

$$\sigma_Z(x=a) \equiv F, = \frac{2}{\sqrt{3}}\bar{\sigma}$$

$$\text{Bridgman Factor} = f_t = \ln\left[1 + \frac{a}{2R}\left(1 - \frac{x^2}{a^2}\right)\right]$$

$$f_t(avg) \equiv \frac{1}{a}\int_0^a f_t\, dx, \quad f_{twa} \equiv 1.4 * f_t(avg) \qquad (15)$$

twa ~ transverse, Wierzbicki / Gao term, avg.

So the stresses and triaxiality are

$$\sigma_X = \frac{2}{\sqrt{3}}\bar{\sigma}\, f_t, \quad \sigma_Y = \frac{2}{\sqrt{3}}\bar{\sigma}\left(\frac{1}{2} + f_t\right),$$
$$\sigma_Z = \frac{2}{\sqrt{3}}\bar{\sigma}\left(1 + f_t\right) \qquad (16)$$
$$\sigma_H = \frac{2}{\sqrt{3}}\bar{\sigma}\left(\frac{1}{2} + f_t\right),$$

$$\eta(avg) = \frac{\sigma_H(avg)}{\bar{\sigma}} = \frac{2}{\sqrt{3}}\left(\frac{1}{2} + f_{twa}\right)$$

The **Butterfly** geometry is modeled as a plane strain geometry, with the load at an angle in the normal-transverse plane. Notch related stresses are due to the normal component of the load. The details of the calculation will appear elsewhere [10].

Stress Invariants, Triaxiality, and Lode Parameter

The damage model is a function of the first three stress invariants, as defined below. Note: A single subscript on stress or strain components indicates principal values, and s_{ij} are deviatoric stresses.

$$\sigma_H = \frac{1}{3}(\sigma_1 + \sigma_2 + \sigma_3), \qquad s_{ij} \equiv \sigma_{ij} - \sigma_H\, \delta_{ij}$$

$$J_2 = \frac{1}{2}s_{ij}\, s_{ij}, \qquad \bar{\sigma} = \sqrt{3J_2}, \qquad \eta = \frac{\sigma_H}{\bar{\sigma}} \qquad (17)$$

$$J_3 = s_1\, s_2\, s_3, \qquad \xi = \frac{27}{2}\frac{J_3}{(\bar{\sigma})^3}$$

Note that the Lode parameter is equal to +1 for axisymmetric tension, 0 for plane strain, and -1 for biaxial tension.

Measures of Plastic Strain

The specimens are cylinders and plates with notches cut in to define the gage sections. The measured variable is equivalent plastic strain to failure at the gage section:

$$\text{Cylinder}: \ \bar{\varepsilon}_f \ = \ \ln\left(\frac{A_0}{A_f}\right) \ = \ 2\ln\left(\frac{D_0}{D_f}\right)$$

D_0 and D_f are initial and final notch diameters (18)

$$\text{Plate (plane strain)}: \ \bar{\varepsilon}_f \ = \ \frac{2}{\sqrt{3}}\ln\left(\frac{t_0}{t_f}\right)$$

t_0 and t_f are initial and final notch thicknesses

Adaptation to Plastic Strain

Given the assumptions for the gage volume, equation 2 can be written as

$$P_S \ = \ \exp\left[-\left(\frac{V}{V_0}\right)\left(\frac{\bar{\varepsilon}_f}{f_1(\eta)\,f_2(\xi)\,\varepsilon_0}\right)^m\right], \qquad (19)$$

where the functions of triaxiality and Lode parameter are not yet specified. They will arise later from combinations of physical reasoning, numerical results, and calibration to physical data.

Start with the simplest case, which is a set of failure strains for a sample of nominally identical specimens. With no variation in volume, and since V_0 is arbitrary, set $V = V_0$. Triaxiality and Lode parameter are also constant. The equation can be written as

$$P_S \ = \ \exp\left[-\left(\frac{\bar{\varepsilon}_f}{\varepsilon_\Theta}\right)^m\right], \qquad (20)$$

where $\varepsilon_\Theta \ = \ f_1(\eta)\,f_2(\xi)\,\varepsilon_0 \ \equiv \ F\varepsilon_0$

The Weibull parameters are m and ε_Θ, which can be found as in equation 6. Different samples made from the same material will likely show some variation in the Weibull modulus m; this variation should diminish as the number of specimens in a sample increases.

Next, consider the case where specimens are geometrically similar, and differ between samples by a length scale. Since triaxiality and Lode parameter are constant, write equation 19 as

$$P_S \ = \ \exp\left[-\left(\frac{V}{V_0}\right)\left(\frac{\bar{\varepsilon}_f}{\varepsilon_\Theta}\right)^m\right] \qquad (21)$$

Equivalent terms for analysis of one sample at a time (equation 6) are

$$\varepsilon_f(i) \ \Leftrightarrow \ X_f(i), \quad \varepsilon_\Theta \ \Leftrightarrow \ X_0, \qquad (22)$$

And for combining several samples,

$$\varepsilon_f(i,k) \ \Leftrightarrow \ X_f(i,k), \qquad (23)$$
$$V \ \Leftrightarrow \ V(k), \quad \varepsilon_\Theta \ \Leftrightarrow \ X_0,$$

When the Weibull parameters are determined, the analysis can be compared to the data by drawing lines of strain vs. geometric scale (e.g., notch diameter) at constant values of P_S. These can be chosen in rough equivalence to + / - 0, 1, and 2 standard deviations.

$$\varepsilon_f \ = \ \varepsilon_\Theta\left[\left(\frac{V_0}{V}\right)\ln\left(\frac{1}{P_S}\right)\right]^{\frac{1}{m}}, \qquad (24)$$
$$P_S \ = \ 0.025, \quad 0.16, \ 0.50, \ 0.84, \ 0.975$$

The work of Young, et. al. [11] meets the data requirements of this case. Ductility was measured for several samples of notched round bars, all geometrically similar, with a different length scale for each sample. So, if L is the diameter at the notch (the notch root diameter),

$$V \ = \ \text{Const.}^* L^3 \qquad (25)$$

Their data (points and sample means) vs. notch root diameter, plus the lines generated using equation 25, are displayed in Figures 2 and 3. Figure 2 uses the Weibull parameters generated by the sample with the largest root diameter. It is interesting that this one sample (with only 5 data points) is so predictive of the other data. The Weibull moduli in Figure 3 were calculated from the combined samples, as per equation 9.

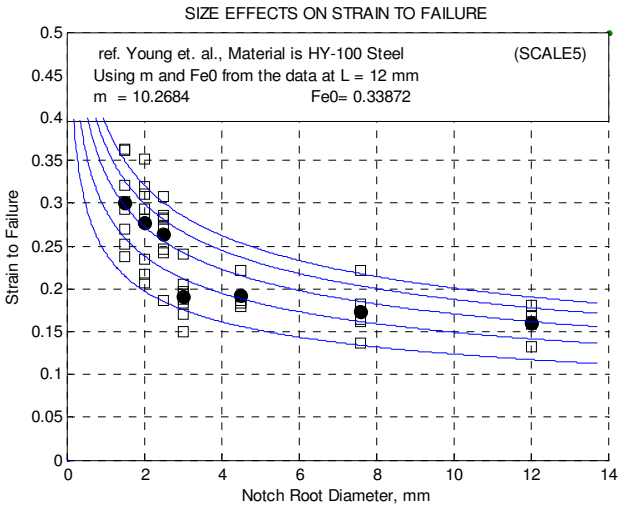

Figure 2. Analysis for Data of Young, et. al., Effect of Scale. Notched Bars, Geometrically Similar. Key on Data from Largest Specimens. Lines are for P_S = 0.023, 0.16, 0.5, 0.84, and 0.977

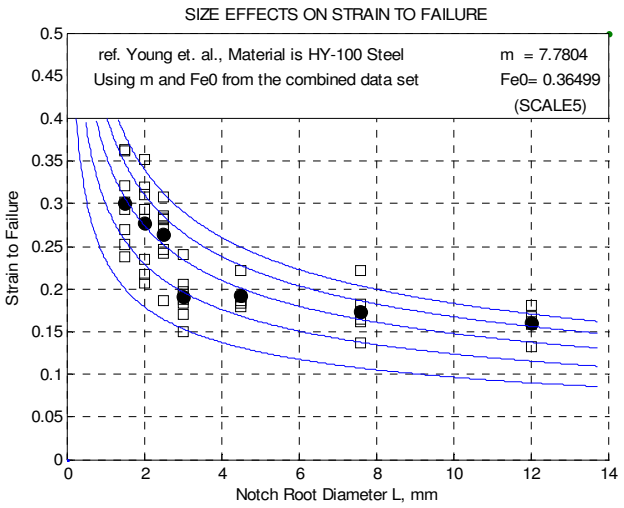

Figure 3. Analysis for Data of Young, et. al. Using All of the Data. Lines are for P_S = 0.023, 0.16, 0.5, 0.84, and 0.977

As shown by equations 12 and 15, triaxiality is determined by the ratio (a / R). The effect of triaxiality on ductility is assumed to be an exponential decay, as shown in equation 2. In order to calibrate the equation, data at several different values of triaxiality, with constant Lode parameter, is required. This can be done by using round tensile bars with a different notch profile for each sample. As shown below, the process requires a fixed value of the Weibull modulus m, which can be an average of the values for each sample. From equations 19 and 2,

$$P_S = \exp\left[-\left(\frac{V}{V_0}\right)\left(\frac{\bar{\varepsilon}_f}{\exp(-C\eta) f_2(\xi)\varepsilon_0}\right)^m\right], \qquad (26)$$

which can be linearized to

$$\left\{\frac{1}{m}\left[\ln\ln\left(\frac{1}{P_S}\right) - \ln\left(\frac{V}{V_0}\right)\right] - \ln\left(\bar{\varepsilon}_f\right)\right\} = C\eta - \ln\left(f_2\,\varepsilon_0\right) \qquad (27)$$

Arrange $\bar{\varepsilon}_f(i,k)$ and Compute $P_S(i,k)$ as before.

Then $Y2(i,k)$ = (28)

$$\left\{\frac{1}{m}\left[\ln\ln\left(\frac{1}{P_S(i,k)}\right) - \ln\left(\frac{V(k)}{V_0}\right)\right] - \ln\left(\bar{\varepsilon}_f(i,k)\right)\right\}$$

And $X(i,k) = \eta(k)$

Least square regression fit of

$Y2(i,k)$ vs. $X(i,k)$ to $Y = a + bX$ $\rightarrow$ (29)

$C = b$, $-\ln(f_2\,\varepsilon_0) = a$, $f_2\,\varepsilon_0 = \exp(-a)$

The data presented by Besson, et. al. [12] contains both types of data discussed so far: geometrically similar with

varying scale, and varying triaxiality. Strain to failure vs. initial triaxiality for six samples is shown in Figure 4. The three that are geometrically similar have the same triaxiality, but due to their different length scales have different mean values of strain to failure.

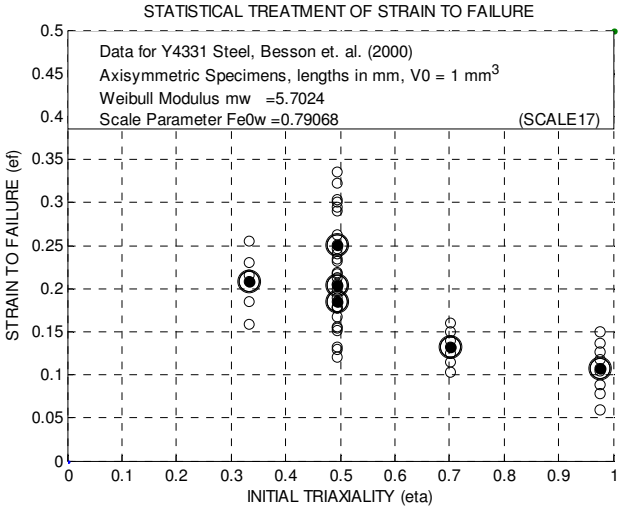

Figure 4. Data from Besson (2000). Small Circles are Data Points, Large Circles are Sample Means.

Equation 26 can be rewritten as follows;

$$P_S = \exp\left[-\left(\frac{\bar{\varepsilon}_{f4}}{\exp(-C\eta) f_2 \varepsilon_0}\right)^m\right], \qquad (30)$$

$$\text{Where } \bar{\varepsilon}_{f4} = \bar{\varepsilon}_f \left(\frac{V}{V_0}\right)^{\frac{1}{m}}$$

This suggests that if the formulation is correct, $\bar{\varepsilon}_{f4}$ can be considered as a volume adjusted strain, and using it should close the gap between the three mean values at the same triaxiality in Figure 4. This is tested in Figure 5, where the data points are replotted as volume adjusted strain, and lines of constant P_S are drawn according to

$$\bar{\varepsilon}_{f4} = \exp(-C\eta) f_2 \varepsilon_0 \left[\ln\left(\frac{1}{P_S}\right)\right]^{\frac{1}{m}} \qquad (31)$$

Note that the three mean values are drawn closer together, and that the lines are consistent with the data.

If a form can be written for $f_2(\xi)$, it should be possible to directly compare data for different Lode parameters. Equation 32 is a further revision of equation 26;

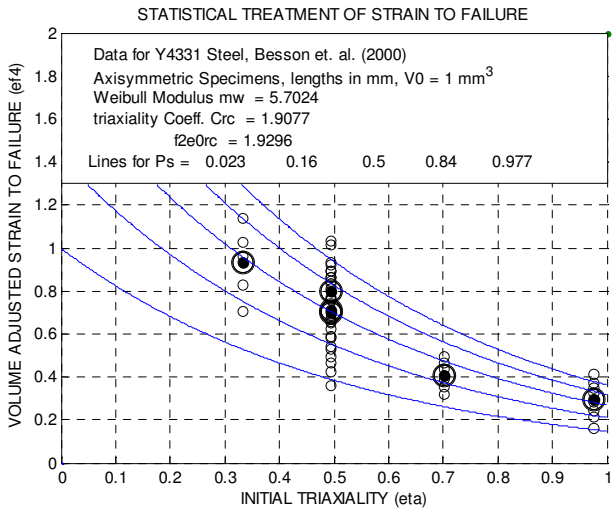

Figure 5. Volume Adjusted Strain vs. Triaxiality.

$$P_S = \exp\left[-\left(\frac{\bar{\varepsilon}_{f5}}{\exp(-C\eta)\varepsilon_0}\right)^m\right], \qquad (32)$$

$$\text{Where } \bar{\varepsilon}_{f5} = \frac{\bar{\varepsilon}_{f4}}{f_2(\xi)}$$

An approximate form of $f_2(\xi)$ was obtained by fitting an equation to some numerical data. In a recent paper, Gao, et. al. [13] presented a finite element analysis of a unit cell with a void at the center, subject to various stress ratios, and an instability criterion related to plastic flow. The variation of failure strain with Lode parameter is consistent with the following approximation:

$$f_2(\xi) = \sqrt{\frac{3}{2+\xi}} \qquad (33)$$

(Other assumptions could lead to different results, such as a constant value of 1 (no dependence on Lode parameter).

Data with variation in specimen type, and triaxiality and Lode parameter, is presented by Mae et. al. [14]. Specimen types include Butterfly, and notched and smooth tensile bars. Specimen failures are matched to finite element calculations, and data reported as plastic strain and triaxiality at a location close to the observed failure. See Figure 6. Note the overlap between specimen types, and the somewhat uncertain dependence of strain to failure on triaxiality.

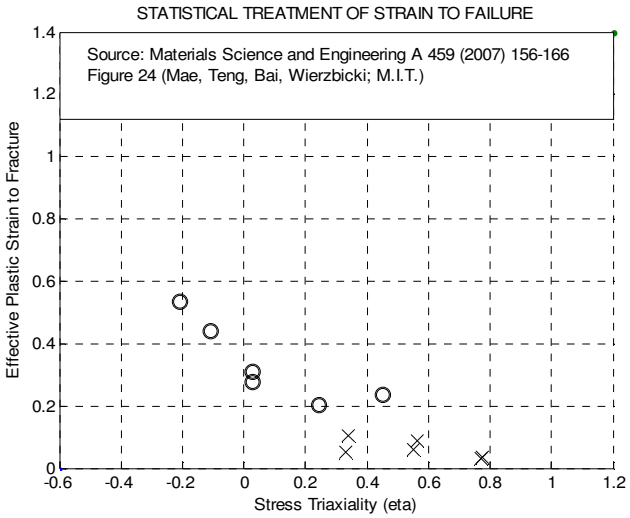

FIGURE 6. X = Axisymmetric, O = Butterfly. Failure Point Strain vs. Failure Point Triaxiality.

Recast the data as follows: Use the initial triaxiality as calculated from the specimen geometry. Keep the reported strain data; assume it is roughly proportional to what would result using reduction of area. Adjust the strains for gage volume and Lode parameter as per equations 32 and 33. Because the samples do not contain enough points for valid statistical calculations, try several values of Weibull modulus and choose one that gives sensible results. Compute lines of $\bar{\varepsilon}_{f5}$ at constant P_S using equation 32. These results are presented in Figure 7. Note the improved consistency.

It is generally expected that increased strain rate results in decreased ductility. Some confusion on this issue was expressed in regard to measurements on Weldox 460 E steel [15-17]. The authors state that results for unnotched round bars showed the expected strain rate response (2001), while those for notched bars did not (2003). Data is given for ductility vs. the maximum initial triaxiality (at the centerline of notched bars); average values only for low (quasi-static) strain rate, and data points for higher strain rates. High strain rates were achieved using Hopkinson bars that were preloaded, and then released into the specimens. The data is shown in Figures 8 and 9:

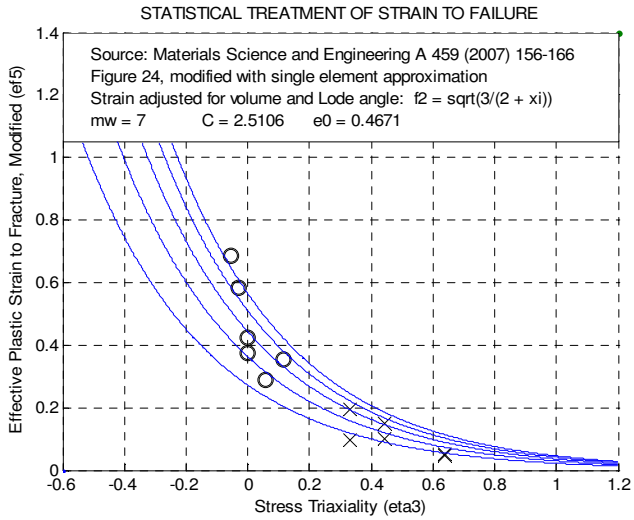

Figure 7. Modified Strain vs. Initial Triaxiality. Lines are for P_S = 0.023, 0.16, 0.5, 0.84, and 0.977

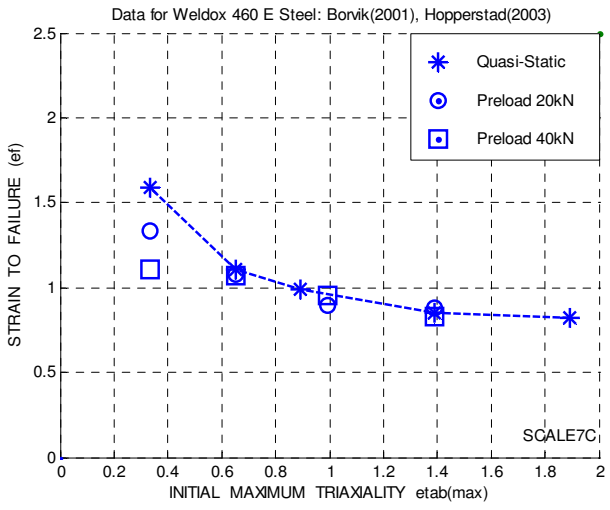

Figure 8. Strain Rate and Triaxiality. Several Strain Rates. Averages of Data Points at Each Condition.

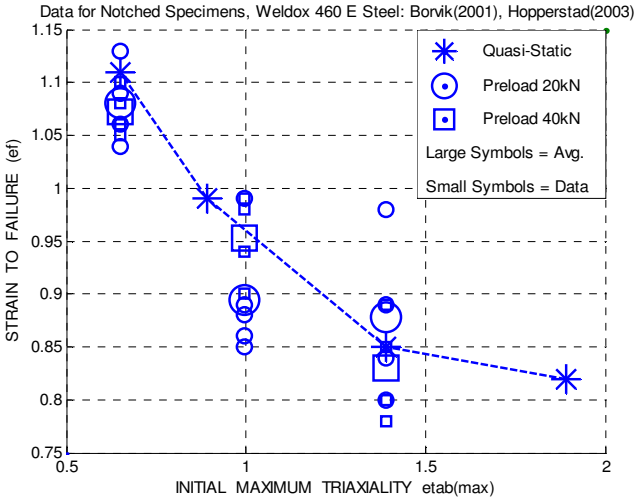

Figure 9. Notched Specimens Only. Several Strain Rates. Data Points and Averages.

A plausible explanation was found when the specimen geometries were examined. For the notched specimens, the notch diameter of the quasi-static specimens was twice that of the dynamic specimens, so the gage volume was approx. 8 times larger. This was combined with an assumed Weibull modulus value of 15, and volume corrected values of the strains were calculated. See Figure 10. Note the separation between the high and low strain rate data, with the high strain rate data having the expected lower strain to failure results.

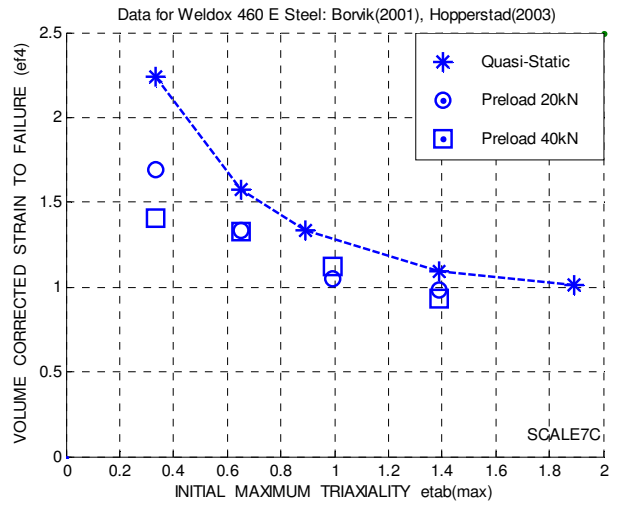

Figure 10. Strain Rate and Triaxiality. Average Values of Volume Corrected Strains vs. Initial Triaxiality. Volume Correction Uses Weibull Modulus = 15.

DISCUSSION / SUMMARY

A statistics-based damage model has been proposed that accounts for both scale effects and scatter. These factors become part of the material behavior, and are not related to testing or specimen preparation. Several cases from the literature were examined. The new damage model is shown to resolve some questionable and inconsistent patterns in the data, notably those related to effects of triaxiality on limit strain.

It is suggested that future test programs in this area use sample numbers higher than was found in these examples. At least 12 specimens per sample are recommended. Even with sample sizes smaller than ideal, useful results were obtained.

It is recognized that the statistical nature of limit strains, and the resulting connection to scale effects, has been the subject of other work. Kieselbach and Krieg [18] apply Weibull statistics separately to limit strain data for several groups of identical and geometrically similar specimens. Dorum et. al. [19] use a volume term and Weibull modulus to alter the statistical distribution failure parameters applied to integration points in a finite element model of a test specimen.

A program report is in preparation [10].

REFERENCES

[1] A.L. Gurson, "A Statistics-Based Damage Model that Accounts for Geometric Scale and is Not Sensitive to Grid Size", www.ctc.com, Technology Corner, posted March 2010.

[2] G.R. Johnson and W.H. Cook, "Fracture characteristics of three metals subjected to various strains, strain rates, temperatures and pressures", Engineering Fracture Mechanics, Volume 21, Issue 1, 1985, Pages 31-48.

[3] W. Weibull, "A Statistical Distribution Function of Wide Applicability," Journal of Applied Mechanics, Sept. 1951, pp. 293-297.

[4] ASTM C 1239, "Standard Practice for Reporting Uniaxial Strength Data and Estimating Weibull Distribution Parameters for Advanced Ceramics". (Note: Used here to document Weibull distribution with size scaling. Substitute strain to failure for uniaxial strength.)

[5] E.V. Zaretsky, ed., "MMC Life System Development (Phase I) – A NASA / Pratt & Whitney Life Prediction Cooperative Program", NASA Reference Publication 1361, November 1996. Chapter 7, "Probabilistic Failure Prediction of SCS-6/Ti-15-3 MMC Ring"

[6] P.W. Bridgman, Studies in Large Plastic Flow and Fracture, first ed., McGraw-Hill, 1952.

[7] Y. Bao and T.Wierzbicki, "On the cut-off value of negative triaxiality for fracture", Engineering Fracture Mechanics 72 (2005), pp. 1049-1069.

[8] X. Gao, private communications, April 2008 to the present.

[9] S. M. Selby, ed., CRC Standard Mathematical Tables, 15th Edition, The Chemical Rubber Company, 1967.

[10] A.L. Gurson, "Advanced Combatant Materials: Statistical Analysis of Failure Strain Data", Concurrent Technologies Corporation, in preparation.

[11] C.J. Young, D.A. Koss, and R.K. Everett, "Specimen Size Effects and Ductile Fracture of HY-100 Steel", Communications, Metallurgical and Materials Transactions, vol. 33A, October 2002, pp. 3293 – 3295. (Note – work done at Penn State, sponsored by ONR.)

[12] J. Besson, L. Devillers-Guerville, and A. Pineau, "Modeling of Scatter and Size Effect in Ductile Fracture: Application to Thermal Embrittlement of Duplex Stainless Steels," Engineering Fracture Mechanics, vol. 67 (2000), pp. 169-190.

[13] X. Gao, G. Zhang, and C. Roe, "A Study on the Effect of the Stress State on Ductile Fracture", International Journal of Damage Mechanics, Vol. 19, No. 1, 75-94 (2010).

[14] H. Mae, X. Teng, Y. Bai, and T. Wierzbicki, "Calibration of Ductile Fracture Properties of a Cast Aluminum Alloy," Materials Science and Engineering A 459 (2007) 156-166.

[15] T. Borvik, O.S. Hopperstad, T. Berstad, and M. Langseth, "A computational model of viscoplasticity and ductile damage for impact and penetration", European Journal of Mechanics A/Solids 20 (2001), pp. 685-712.

[16] O.S. Hopperstad, T. Borvik, M. Langseth, K. Labibes, and C. Albertini, "On the influence of stress triaxiality and strain rate on the behavior of structural steel. Part I. Experiments", European Journal of Mechanics A/Solids 22 (2003), pp. 1-13.

[17] T. Borvik, O.S. Hopperstad, T. Berstad, "On the influence of stress triaxiality and strain rate on the behavior of structural steel. Part II. Numerical Study", European Journal of Mechanics A/Solids 22 (2003), pp. 15-32.

[18] R. Kieselbach and R. Krieg, "Size Effect in Strain Limits of Medium Strength Steel", Journal of Testing and Evaluation, September 2005, Vol. 33, No. 5.

[19] C. Dorum, D. Dispinar, O.S. Hopperstad, and T. Berstad, "A Probabilistic Approach for Modelling of Fracture in Magnesium Die-Castings", Italian Metallurgy (la metallurgia italiana), March 2009, pp. 51-54.